materials proceedings

MDPI

Proceeding Paper

Electron-Beam Radiation Effects in Multilayer Structures Grown with the Periodical Deposition of Si and CaF_2 on Si(111) †

Anatoly V. Dvurechenskii [1,2,*], Aleksey V. Kacyuba [1], Gennady N. Kamaev [1], Vladimir A. Volodin [1,2], Natalia P. Stepina [1], Aigul F. Zinovieva [1,2] and Vladimir A. Zinovyev [1]

1 Rzhanov Institute of Semiconductor Physics, Siberian Branch of Russian Academy of Sciences, 630090 Novosibirsk, Russia; kacyuba@isp.nsc.ru (A.V.K.); kamaev@isp.nsc.ru (G.N.K.); volodin@isp.nsc.ru (V.A.V.); stepina@isp.nsc.ru (N.P.S.); aigul@isp.nsc.ru (A.F.Z.); zinoviev@isp.nsc.ru (V.A.Z.)
2 Department of Physics, Novosibirsk State University, 630090 Novosibirsk, Russia
* Correspondence: dvurech@isp.nsc.ru
† Presented at the 4th International Online Conference on Nanomaterials, 5–19 May 2023; Available online: https://iocn2023.sciforum.net.

Abstract: The formation of $CaSi_2$ films on Si(111) with the molecular-beam epitaxy (MBE) of CaF_2 under fast electron-beam irradiation was investigated. The method of a high-planarity $CaSi_2$ film synthesis assisted by electron-beam irradiation was developed. We combined two approaches to reduce the film roughness: the post-growth electron irradiation and codeposition of additional Si during CaF_2 growth. The application of the solid-phase epitaxy technique at the initial stage of film growth allowed for us to reduce surface roughness down to 1–2 nm.

Keywords: crystal structure; nanostructures; electron-beam radiation; molecular-beam epitaxy; calcium compounds; silicon

check for updates

Citation: Dvurechenskii, A.V.; Kacyuba, A.V.; Kamaev, G.N.; Volodin, V.A.; Stepina, N.P.; Zinovieva, A.F.; Zinovyev, V.A. Electron-Beam Radiation Effects in Multilayer Structures Grown with the Periodical Deposition of Si and CaF_2 on Si(111). *Mater. Proc.* **2023**, *14*, 68. https://doi.org/10.3390/IOCN2023-14481

Academic Editor: José Luis Arias Mediano

Published: 5 May 2023

Copyright: © 2023 by the authors. Licensee MDPI, Basel, Switzerland. This article is an open access article distributed under the terms and conditions of the Creative Commons Attribution (CC BY) license (https://creativecommons.org/licenses/by/4.0/).

1. Introduction

CaF_2 and $CaSi_2$ materials have a slight difference in the parameters of the crystal lattice with silicon [1] that allows for the epitaxial growth of the multilayer heterostructures based on these materials on silicon substrates. The possibility of obtaining multilayer structures with conducting $CaSi_2$ layers separated by a CaF_2 dielectric can be used for the development of future nanoelectronic devices. There are quite a few works devoted to the study of this system. Calcium silicide films obtained on Si(111) and Si(001) surfaces can have different phase compositions. With the simultaneous deposition of Ca and Si on a hot substrate with increasing temperature, a phase tends to form with the highest silicon content, i.e., Ca_2Si–CaSi–$CaSi_2$. Ca_2Si films are narrow-band semiconductor materials, and CaSi and $CaSi_2$ films are semimetals. On the basis of these silicides, approaches to obtaining materials with various functional properties are being developed [1–13]. Recently, we proposed a method for $CaSi_2$ synthesis using electron-beam irradiation during the growth of CaF_2 layers with molecular-beam epitaxy (MBE) [14,15]. The method is based on the electron-beam-stimulated decomposition of CaF_2 into Ca and F [16] in the surface layers. Fluorine is desorbed from the surface, and the remaining calcium atoms bind chemically with silicon atoms that come from the Si substrate at sufficiently high temperatures (>300 °C) under electron irradiation [9]. Calcium silicide produced in this way is a nonhomogeneous three-dimensional material representing a triangular network of elongated crystallites protruding from the surface of the CaF_2 film by tens of nanometers. These crystallites are oriented along the {110} directions and have a characteristic length of ~1 μm. The situation is similar to that of $CaSi_2$ films grown by Braungart and Sigmund [17], who exposed a heated Si substrate to Ca vapor. We recently found a way to produce more homogeneous $CaSi_2$

films [18]. The idea is to introduce additional intermediate silicon layers into the growing CaF_2 film. The preliminary results showed that, under certain conditions, $CaSi_2$ film growth under simultaneous e-beam irradiation can occur in a layer-by-layer mode. In addition, we tested another opportunity to increase the $CaSi_2$ film homogeneity via post-growth electron irradiation after CaF_2 deposition [19]. So far, however, there has been no notable success in this direction. Both types of structures, obtained with electron irradiation during CaF_2 epitaxial growth and after CaF_2 film formation, revealed the problem of high surface roughness. The average surface roughness in the irradiated region is 6–8 nm for films irradiated during CaF_2 film growth, and 25–30 nm for films formed with post-growth irradiation (the values are given for the same thickness of the deposited film, irradiation dose, and substrate temperature). These data indicate that the considered methods do not provide the necessary planarity of $CaSi_2$ epitaxial films.

The purpose of this work is to develop the synthesis method of a high-planarity $CaSi_2$ film assisted by electron-beam irradiation. We combined two approaches to reduce the film roughness, a post-growth electron irradiation and codeposition of additional Si during CaF_2 growth. Following Morar and Wittmer [1,20], we applied the technique of solid-phase epitaxy with subsequent annealing at the initial stage of film growth that allowed for us to reduce surface roughness down to 1–2 nm.

2. Materials and Methods

The experiments were carried out on a Katun-100 molecular-beam epitaxy (MBE) unit equipped with a CaF_2 effusion source with a graphite crucible under ultrahigh vacuum conditions. Films were grown on an Si(111) substrate. For all samples, the standard procedure of double surface cleaning was performed before the growth [18]. The crystal structure of the deposited layers was studied via the rapid high-energy electron diffraction (RHEED) method. Electron-beam irradiation was performed with accelerating voltage of 20 Kev and current density of 50 $\mu A/cm^2$. The beam incidence angle was 4°. The same electron beam was used to modify the properties of the growing film. Epitaxial CaF_2 film growth was carried out at a deposition rate of 0.3 Å/s and consisted of two steps. At the first step, a 2 nm thick CaF_2 layer was deposited at room temperature. Then, this amorphous layer was crystallized via annealing at 700 °C. The crystallization process was controlled with RHEED. At the second step, a multilayer structure containing 10 Si layers with 1 nm thickness separated by 2 nm thick CaF_2 layers was grown at 550 °C. At the top of this structure, a 2 nm thick CaF_2 layer was deposited. At the next step, structures were subjected to post-growth electron irradiation with different exposure times (10, 20, and 60 min). During post-growth irradiation, the electron beam did not shift, that is, the same area was irradiated as during growth. The thickness of the grown films was controlled with ellipsometry. The phase composition was determined on the basis of the Raman light scattering method. Surface morphology was studied using atomic force microscopy (AFM) and scanning electron microscopy (SEM). To highlight the effect of silicon codeposition on the resulting smoothing effect of the film, we carried out a test experiment in which we grew the film under the same growth conditions, but without silicon codeposition. Conductivity and magnetoresistance were measured on the strips as a function of the post-growth electron irradiation time. Contacts for the transport measurements were created by soldering silver wires using an indium solder. The temperature dependences of the conductivity were measured using an SR850 synchronous amplifier in a transport helium Dewar vessel. Magnetoresistance was measured in a magnetic field of up to 4 T.

3. Results and Discussion

RHEED studies confirmed that annealing at 700 °C leads to the recrystallization of CaF_2 film deposited at room temperature (Figure 1a,b). RHEED data demonstrate that the further growth of a multilayer structure at 550 °C under electron irradiation resulted in the formation of a crystalline film (Figure 1c). Post-growth irradiation for 10 and 20 min did not induce any changes in RHEED images, while longer electron exposure led to additional RHEED reflexes, indicating a change in surface reconstruction (Figure 1d).

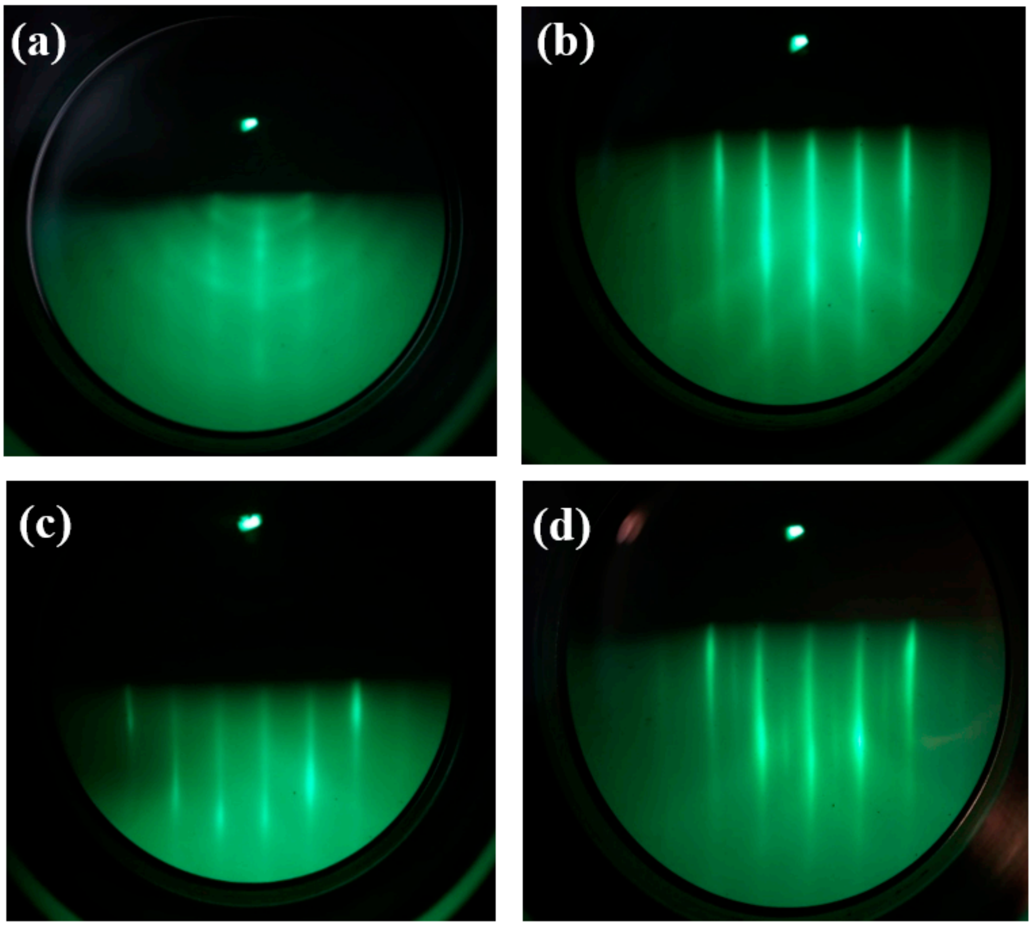

Figure 1. (**top**) RHEED images of the surface of a 2 nm thick CaF_2 film deposited at room temperature. (**a**) As-grown 2 nm thick CaF_2 film; (**b**) after annealing at 700 °C. (**bottom**) RHEED images of multilayer structure with additional 2 nm thick Si cap layer (**c**) just after growth and (**d**) after 60 min post-growth electron irradiation.

The AFM and SEM studies of the first type of structure show that, in the chosen growth conditions (codeposition of additional Si during CaF_2 growth under electron irradiation), flat, hexagonal islands of $CaSi_2$ formed instead of elongated crystallites. The characteristic size of the islands was ~300–400 nm. The post-growth irradiation led to an increase in the number and size of islands. Figure 2 demonstrates the SEM images of the surface of the as-grown film and after post-growth irradiation. An increase in irradiation dose clearly led to the islands overlapping and having a tendency to form a continuous film. However, if the exposure time was too long, the surface relief changed, and the film became less planar due to the appearance of three-dimensional ripples. For example, after 60 min irradiation, the average surface roughness was 6 nm. Results of AFM studies (Figure 3) show that the best planarity (lowest surface roughness ≈1 nm) was obtained for films with 20 min electron irradiation.

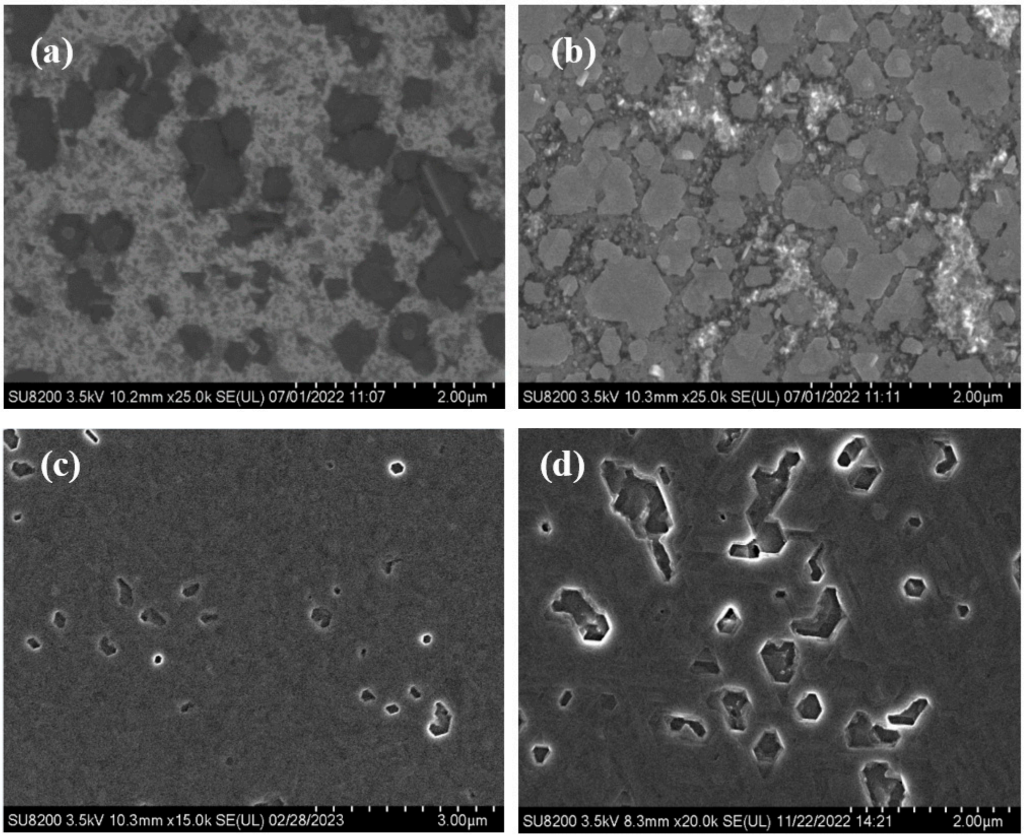

Figure 2. SEM images of surface of (**a**) as-grown CaF_2 film, (**b**) after 10 min post-growth electron irradiation, (**c**) after 20 min post-growth electron irradiation, (**d**) after 60 min post-growth electron irradiation.

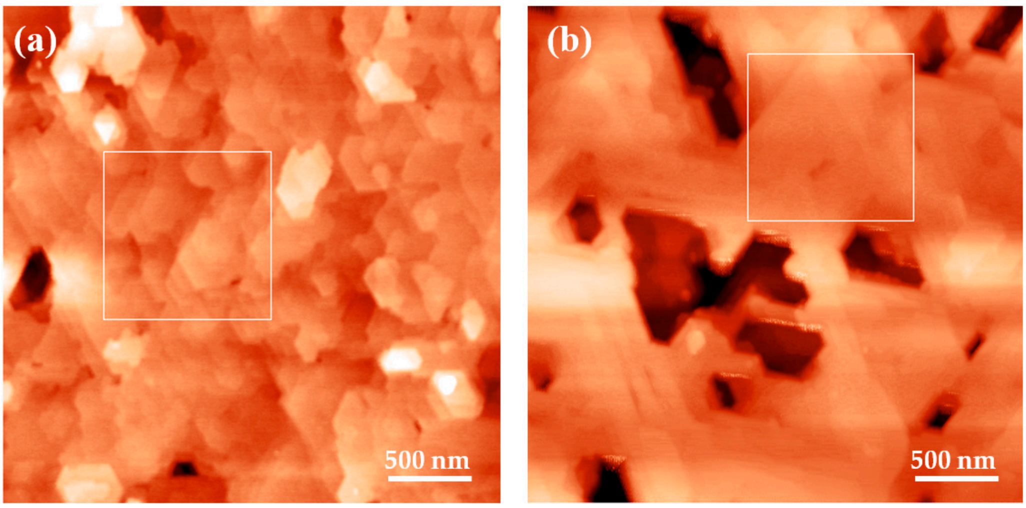

Figure 3. AFM images of the film synthesized with (**a**) post-growth electron irradiation during 20 min and (**b**) with 60 min post-growth electron irradiation. Height parameters in selected areas (white squares 1 μm × 1 μm): root mean square height Sq ≈ 1.07 nm for (**a**) and Sq ≈ 7.7 nm for (**b**); surface skewness Ssk ≈ −0.007 for (**a**) and Ssk ≈ 0.51 for (**b**); coefficient of kurtosis Sku ≈ −0.42 for (**a**) and Sku ≈ 0.17 for (**b**); arithmetic mean height Sa ≈ 0.87 nm for (**a**) and Sa ≈ 6.1 nm for (**b**). If one consider the whole area of the images, the parameters are as follows: Sq ≈ 2.1 nm for (**a**) and Sq ≈ 17.8 nm for (**b**); Ssk ≈ 0.27 for (**a**) and Ssk ≈ −1.67 for (**b**); Sku ≈ 5.21 for (**a**) and Sku ≈ 6.5 for (**b**); Sa ≈ 1.4 nm for (**a**) and Sa ≈ 11.7 nm for (**b**).

The test experiment in which we grew the film in the same growth conditions but without Si codeposition demonstrates that the exclusion of Si codeposition resulted in worse film planarity. For the film obtained after a 20 min post-growth electron irradiation, the average surface roughness increased up to 5–6 nm. This result is in agreement with existing literature data on $CaSi_2$ growth via calcium deposition on Si substrates. Vogg et al. [21] reported that, by increasing the calcium flux and lowering the substrate temperature, one can achieve selective growth in the preferential direction and essentially switch from two- to three-dimensional growth. In our case, calcium was supplied in the process of radiolysis of CaF_2 film, and silicon was supplied by diffusion from the substrate (under conditions without additional silicon deposition), and the situation is similar to that of growth in Vogg conditions with a large calcium flux, i.e., a three-dimensional growth mode was realized. If we deposited additional silicon, we would change the ratio of calcium and silicon, in fact reducing the effective calcium flux and changing the growth mode into a two-dimensional one, which was observed in our experiments.

The Raman measurements of samples in the irradiated regions gave spectra with three typical peaks of $CaSi_2$ layers (Figure 4) obtained via electron irradiation during CaF_2 MBE ($CaSi_2$ polymorph 3R) [15]. In addition, the longer the exposure time was, the higher the intensity of the peaks was. Earlier, we observed such spectra on $CaSi_2$ films synthesized under electron irradiation, but without an additional peak at 430 cm^{-1}. Since the appearance of this peak correlates with a presence of boundaries between $CaSi_2$ regions and residual inclusions CaF_2, we attribute it to scattering at the boundaries of $CaSi_2$ formations.

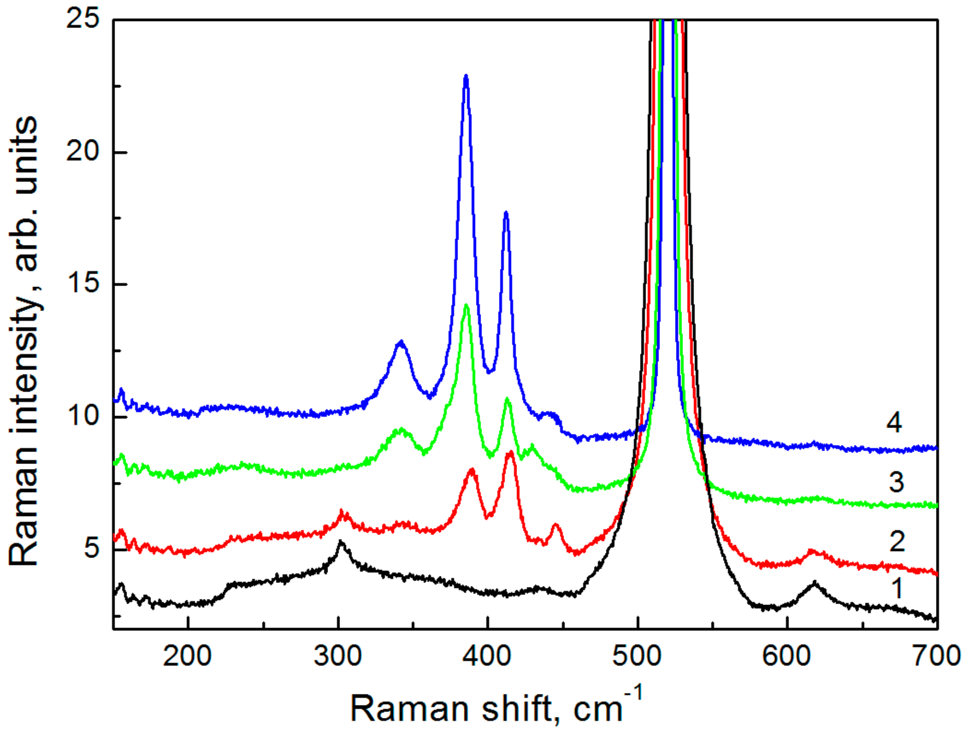

Figure 4. Raman spectra of films synthesized with different processing types. (2) Post−growth electron irradiation during 20 min; (3) post-growth electron irradiation during 10 min; (4) post-growth electron irradiation during 60 min. Spectrum (1) was obtained on a Si(111) substrate.

Figure 5 demonstrates temperature dependence of conductance for three films grown under the same growth conditions, but with different time of post-growth irradiation. The increase im irradiation time from 10 to 60 min led to an increase in film conductivity that corresponded to the increase in lateral island size and their overlapping observed in the SEM study (Figure 1). Magnetoresistance (MR) data for these films are shown in the inset of Figure 5. Non-monotonic MR behavior with a transition from negative to positive MR was observed for all samples, with the larger contribution of positive MR for the longer irradiation time. A negative MR is usually associated with the suppression of weak localization that is typical of disordered electronic systems with low mobility. A positive MR is the result of the Lorentz deflection of the carriers [22] and also depends on carrier mobility: $(B)/R(B = 0) \sim 1 + (\mu B)^2$ (Kohler's rule [23]). This allows for estimating mobility μ, which was 158 cm^2/Vs for Sample 1, 230 cm^2/Vs for Sample 2, and 330 cm^2/Vs for Sample 3. These results support the structural data and indicate that the increase in irradiation time rendered the samples more metallic.

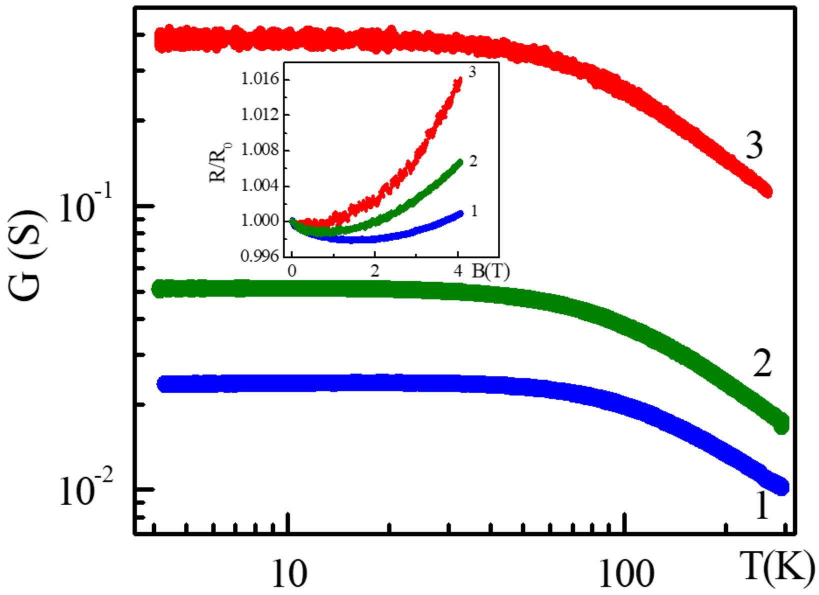

Figure 5. Temperature dependence of conductivity G for three films synthesized with different post-growth irradiation times (1-10 min, 2-20 min, and 3-60 min). Inset demonstrates the magnetoresistance of these films.

4. Conclusions

A study of the structural properties of the grown samples confirmed that the developed approach could solve the problem of high surface roughness. The use of the solid-phase epitaxy method at the initial growth stage enabled the formation of a thin Ca-enriched layer under electron irradiation. By supplying additional Si to this surface, one can form $CaSi_2$ two-dimensional islands parallel to the (111) surface of the substrate. Post-growth electron irradiation led to an increase in the number and size of islands. An increase in irradiation dose resulted in overlapping islands and a tendency to form a continuous film. However, if the exposure time was too long, the surface relief changed, and the film became less planar due to the appearance of three-dimensional ripples. The best planarity (lowest surface roughness) was obtained after 20 min post-growth irradiation. The conductivity for the synthesized $CaSi_2$ films increased by increasing the time of post-growth electron irradiation.

Author Contributions: Conceptualization, A.F.Z., V.A.Z. and A.V.D.; investigation, A.F.Z., V.A.Z., N.P.S., V.A.V., G.N.K. and A.V.K.; methodology, A.V.K.; supervision, A.V.D.; visualization, A.F.Z. and N.P.S.; writing—original draft, A.F.Z., V.A.Z. and N.P.S.; writing—review and editing, A.V.D. All authors have read and agreed to the published version of the manuscript.

Funding: The work is funded by the Russian Science Foundation (grant no. 19-12-00070-П).

Institutional Review Board Statement: Not applicable.

Informed Consent Statement: Not applicable.

Data Availability Statement: Data are contained within the article.

Acknowledgments: The authors thank NSU Multiple-Access Center VTAN and ISP SB RAS Multiple-access Center Nanostructures for the provision of the measurement equipment.

Conflicts of Interest: The authors declare no conflict of interest.

References

1. Morar, J.F.; Wittmer, M. Growth of epitaxial $CaSi_2$ films on Si(111). *J. Vac. Sci. Technol. A* **1988**, *6*, 1340. [CrossRef]
2. Galkin, N.G.; Galkin, K.N.; Dotsenko, S.A.; Goroshko, D.L.; Fogarassy, Z.; Pecz, B. The growth processes and crystal structure of Ca silicides films grown by MBE at 500 °C on a Si(001) substrate. *Mater. Chem. Phys.* **2020**, *253*, 123380. [CrossRef]
3. Galkin, N.G.; Galkin, K.N.; Tupkalo, A.V.; Chusovitin, E.A.; Goroshko, D.L.; Fogarassi, Z.; Pecz, B. Semitransparent and conductive $CaSi_2$ films for silicon device applications. *Jpn. J. Appl. Phys.* **2020**, *59*, SFFA12. [CrossRef]
4. Galkin, N.G.; Galkin, K.N.; Tupkalo, A.V.; Fogarassy, Z.; Pecz, B. A low temperature growth of Ca silicides on Si(100) and Si(111) substrates: Formation, structure, optical properties and energy band structure parameters. *J. Alloys Compd.* **2020**, *813*, 152101. [CrossRef]
5. Affronte, M.; Laborde, O.; Olcese, G.L.; Palenzona, A. Low temperature properties of calcium mono-and disilicides. *J. Alloys Compd.* **1998**, *274*, 68. [CrossRef]
6. Galkin, N.G.; Galkin, K.N.; Tupkalo, A.V.; Dotsenko, S.A.; Fogarassi, Z.; Pecz, B. Ca Silicide Films on Si(100) and Si(111) Substrates: Structure, Optical and Electrical Properties. *Int. J. Nanosci.* **2019**, *18*, 1940014. [CrossRef]
7. Ohsuna, T.; Ito, K.; Nakano, H. Transformation of CaSi overgrowth domains to the $CaSi_2$ crystal phase via vacuum annealing. *Jpn. J. Appl. Phys.* **2021**, *61*, 025506. [CrossRef]
8. Terada, T.; Ishibe, T.; Katayama, T.; Sato, K.; Nguyen, T.Q.; Nakano, H.; Nakamura, Y. Thermoelectric power factor enhancement of calcium-intercalated layered silicene by introducing metastable phase. *Appl. Phys. Express* **2021**, *14*, 115505. [CrossRef]
9. Kacyuba, A.; Dvurechenskii, A.; Kamaev, G.; Volodin, V.; Krupin, A. Crystal structure of thin $CaSi_2$ films grown by radiation induced epitaxy. *J. Crystal Growth* **2021**, *562*, 126080. [CrossRef]
10. Terada, T.; Uematsu, Y.; Ishibe, T.; Naruse, N.; Sato, K.; Nguyen, T.Q.; Kobayashi, E.; Nakano, H.; Nakamura, Y. Giant Enhancement of Seebeck Coefficient by Deformation of Silicene Buckled Structure in Calcium-Intercalated Layered Silicene Film. *Adv. Mater. Interfaces* **2022**, *9*, 2101752. [CrossRef]
11. Ito, K.; Suemasu, T.; Nakano, H. Growth of tr6-$CaSi_2$ thin films on Si(111) substrates. *Jpn. J. Appl. Phys.* **2018**, *57*, 120313. [CrossRef]
12. Ito, K.; Ohsuna, T.; Suemasu, T.; Nakano, H. Growth and fluorination of $CaSi_2$ thin film. *Jpn. J. Appl. Phys.* **2020**, *59*, SFFC02. [CrossRef]
13. Würz, R.; Schmidt, R.; Schöpke, A.; Fuhs, W. Solid-phase epitaxy of $CaSi_2$ on Si(111) and the Schottky-barrier height of $CaSi_2$/Si(111). *Appl. Surf. Sci.* **2002**, *190*, 437–440. [CrossRef]
14. Kacyuba, A.; Dvurechenskii, A.; Kamaev, G.; Volodin, V.; Krupin, A. Radiation-Induced epitaxial $CaSi_2$ film growth at the molecular-beam epitaxy of CaF2 on Si. *Mater. Lett.* **2020**, *268*, 127554. [CrossRef]
15. Dvurechenskii, A.V.; Kacyuba, A.V.; Kamaev, G.N.; Volodin, V.A.; Smagina, Z.V. Radiation-Induced Nucleation and Growth of $CaSi_2$ Crystals, Both Directly during the Epitaxial CaF_2 Growth and after the CaF_2 Film Formation. *Nanomaterials* **2022**, *12*, 1407. [CrossRef] [PubMed]
16. Charles, L.S.; Moddeman, W.E.; Grant, J.T. Electron-beam-induced decomposition of ion bombarded calcium fluoride surfaces. *Appl. Phys. Lett.* **1981**, *52*, 6921.
17. Braungart, R.; Sigmund, H. Formation of magnesium silicide (Mg_2Si) and calcium silicide ($CaSi_2$) layers on single-crystal silicon substrates. *Z. Naturforsch.* **1980**, *35a*, 1268. [CrossRef]
18. Zinovyev, V.A.; Kacyuba, A.V.; Volodin, V.A.; Zinovieva, A.F.; Cherkova, S.G.; Smagina, Z.V.; Dvurechenskii, A.V.; Krupin, A.Y.; Borodavchenko, O.M.; Zhivulko, V.D.; et al. Atomic Structure and Optical Properties of $CaSi_2$ Layers Grown on CaF_2/Si Substrates. *Semiconductors* **2021**, *55*, 808. [CrossRef]
19. Morar, J.F.; Wittmer, M. Metallic $CaSi_2$ epitaxial films on Si(111). *Phys. Rev. B* **1988**, *37*, 2618. [CrossRef] [PubMed]
20. Zinovieva, A.F.; Zinovyev, V.A.; Stepina, N.P.; Volodin, V.A.; Krupin, A.Y.; Kacyuba, A.V.; Dvurechenskii, A.V. Radiation-Stimulated Formation of Two-Dimensional Structures Based on Calcium Silicide. *Nanomaterials* **2022**, *12*, 3623. [CrossRef] [PubMed]
21. Vogg, G.; Zamanzadeh-Hanebuth, N.; Brandt, M.; Stutzmann, M.; Albrecht, M. Preparation and Characterization of Epitaxial $CaSi_2$ and Siloxene Layers on Silicon. *Chem. Mon.* **1999**, *130*, 7. [CrossRef]
22. Ziman, J.M. *Electrons and Phonons: The Theory of Transport Phenomena in Solids*; Clarendon Press: Oxford, UK, 1960.
23. Olsen, J.L. *Electron Transport in Metals*; Interscience: New York, NY, USA, 1962.

Disclaimer/Publisher's Note: The statements, opinions and data contained in all publications are solely those of the individual author(s) and contributor(s) and not of MDPI and/or the editor(s). MDPI and/or the editor(s) disclaim responsibility for any injury to people or property resulting from any ideas, methods, instructions or products referred to in the content.